



Maximizing the Use of Pandora Data for Scientific Applications

Prajjwal Rawat¹, James H. Crawford¹, Katherine R. Travis¹, Laura M. Judd¹, Mary Angelique G. Demetillo¹, Lukas C. Valin², James J. Szykman², Andrew Whitehill², Eric Baumann², Thomas F. Hanisco³

5

¹NASA Langley Research Center, Hampton, VA, 23681, United States

²Environmental Protection Agency Office of Research and Development, Research Triangle Park, NC, 27709, US

³NASA Goddard Space Flight Center, Greenbelt, MD 20771, USA

10 *Correspondence to:* Prajjwal Rawat (prajjwal.rawat@nasa.gov) and James H. Crawford (james.h.crawford@nasa.gov)

Abstract.

As part of the Pandonia Global Network (PGN), Pandora spectrometers are widely deployed
15 around the world. These ground-based, remote-sensing instruments are federated such that they
employ a common algorithm and data protocol for reporting on trace gas column densities and
lower atmospheric profiles using two modes based on direct-sun and sky-scan observations. To
aid users in the analysis of Pandora observations, the PGN standard quality assurance procedure
assigns flags to the data indicating high, medium, and low quality. This work assesses the
20 suitability of these data quality flags for filtering data in the scientific analysis of nitrogen dioxide
(NO₂) and formaldehyde (HCHO), two critical precursors controlling tropospheric ozone
production. Pandora data flagged as high quality assures scientifically valid data and is often more
abundant for direct-sun NO₂ columns. For direct-sun HCHO and sky-scan observations of both
molecules, large amounts of data flagged as low quality also appear to be valid. Upon closer
25 inspection of the data, independent uncertainty is shown to be a better indicator of data quality
than the standard quality flags. After applying an independent uncertainty filter, Pandora data
flagged as medium or low quality in both modes can be demonstrated to be scientifically useful.
Demonstrating the utility of this filtering method is enabled by correlating contemporaneous but
independent direct-sun and sky-scan observations. When evaluated across 15 Pandora sites in
30 North America, this new filtering method increased the availability of scientifically useful data by
as much as 90% above that tagged as high quality. A method is also developed for combining the
direct-sun and sky-scan observations into a single dataset by accounting for biases between the
two observing modes and differences in measurement integration times. This combined data
provides a more continuous record useful for interpreting Pandora observations against other
35 independent variables such as hourly observations of surface ozone. When Pandora HCHO



columns are correlated with surface ozone measurements, data filtered by independent uncertainty exhibits similarly strong and more robust relationships than high-quality data alone. These results suggest that Pandora data users should carefully assess data across all quality flags and consider their potential for useful application to scientific analysis. The present study provides a method for maximizing use of Pandora data with expectation of more robust satellite validation and comparisons with ground-based observations in support of air quality studies.

1 Introduction

The Pandora spectrometer is a ground-based UV-visible (UV-VIS) remote-sensing instrument utilized to validate space-based UV-VIS sensors and understand local air quality (Herman et al., 2009; Wang et al., 2010; Spinei et al., 2018; Tzortziou et al., 2012; Herman et al., 2019; Szykman et al., 2019; Judd et al., 2019; Verhoelst et al., 2021; Di Bernardino et al., 2023). The Pandora instrument was developed to observe column nitrogen dioxide (NO_2) in direct-sun mode, in addition to the more traditional sky-scan observations obtained using multi axial differential optical absorption spectroscopy (MAX-DOAS). Once calibrated, direct-sun observations are less impacted by atmospheric parameters that influence the air mass factor (AMF) and which also cause uncertainty in space-based retrievals, such as the vertical gas profile or surface albedo (Cede et al., 2006; Herman et al., 2009). More recently, Pandora instrument retrievals of column formaldehyde (HCHO) have become available, expanding opportunities to evaluate the importance of both nitrogen oxides (NO_x) and volatile organic compounds (VOCs) as precursors of ozone and secondary aerosol. This was enabled by the removal of instrument components made of Delrin which were discovered to outgas and create interferences in the detection of HCHO (Spinei et al., 2021).

The Pandonia Global Network (PGN) is a NASA and ESA-sponsored ground-based network of Pandora spectrometers supporting in situ and remotely sensed air quality monitoring and satellite validation activities (<https://blickm.pandonia-global-network.org>). The major advantages of the PGN are uniform instrument design, homogeneous calibrations, centralized data monitoring and processing, and real-time data distribution (Herman et al., 2009, 2018; Spinei et al., 2018; Herman et al., 2019; Cede et al., 2021). Pandora instruments are calibrated by NASA Goddard Space Flight Center and deployed to local operators around the world who join the PGN. Consistent retrievals



65 across the network are performed by Luftblick Earth Observation Technologies and are hosted on
the PGN website (Cede et al., 2021). Presently, there are more than 130 Pandora instruments
worldwide and over 60 across the U.S. (Szykman et al., 2019; Chang et al., 2022).

Pandora instruments have provided valuable information on NO₂ retrieval biases from the polar-
orbiting Sentinel-5P TROPOspheric Monitoring Instrument (TROPOMI) (Judd et al., 2020;
70 Verhoelst et al., 2021; Park et al., 2022; Ialongo et al., 2020) and Ozone Monitoring Instrument
(OMI) (Tzortziou et al., 2012; Reed et al., 2015; Herman et al., 2019). The high temporal
availability of Pandora data has allowed for deep investigation of local meteorology on column
NO₂ and how well that is captured by air quality models (Goldberg et al., 2017; Choi et al., 2020;
Tzortziou et al., 2022; Wang et al., 2023; Adams et al., 2023; Tzortziou et al., 2023). The relatively
75 new formaldehyde retrievals from Pandora (Spinei et al., 2018, 2021) are beginning to be
incorporated into model and satellite validation efforts (Herman et al., 2018) and show promise
for characterizing the local ozone photochemical environment (Schroeder et al., 2016; Travis et
al., 2022).

Geostationary satellite observations provide a new challenge in interpreting NO₂ and HCHO
80 columns at unprecedented spatial and temporal scales (Kim et al., 2017; Judd et al., 2018). Pandora
instruments will be the main source of validation data for both NO₂ and HCHO columns for the
Tropospheric Emissions: Monitoring of Pollution (TEMPO) geostationary air quality satellite
launched over the U.S. in 2023 (Szykman and Liu, 2023; Zoogman et al., 2017). Pandora
instruments are also being used to validate the Geostationary Environmental Monitoring
85 Spectrometer (GEMS) satellite retrievals over East Asia (Kim et al., 2023). Given the growing
need for Pandora data to support satellite observations and model development, improved methods
for ensuring data availability and quality are needed. In this work, a data filtering method is
presented for assessing suitability of data beyond the standard quality flags provided by PGN. This
method takes advantage of the independent but contemporaneous measurement modes of Pandora
90 operation (direct-sun and sky-scan) to analyze Pandora data quality and maximize the availability
of data for scientific application.



2 Data and methodology

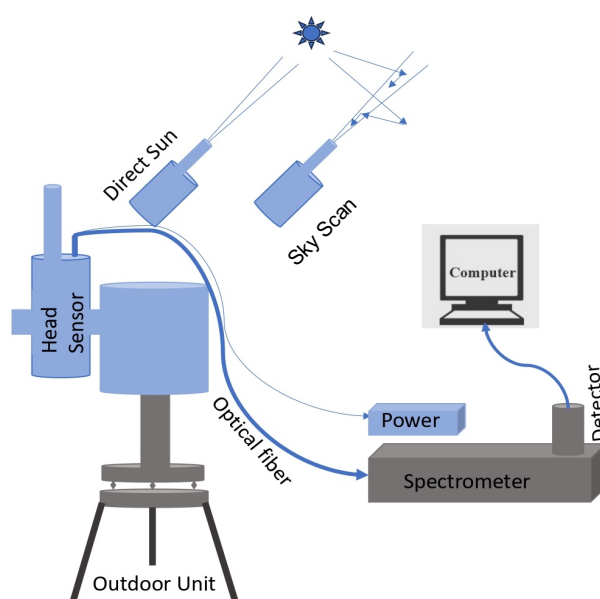
95 2.1 Pandora measurements and data retrieval

The Pandora spectrometer is an instrument for ground-based remote sensing of a range of trace gases, including NO₂, HCHO, O₃, and SO₂, with temporal resolution on the order of seconds to minutes. Pandora is a passive UV-VIS spectrometer system equipped with a responsive sun tracker that points the optical head sensor to the sun or sky with a spatial accuracy of up to ±0.1°. A basic
100 description of the Pandora instrument is summarized here with additional details provided in supplementary section S1.1 and available in Cede et al., (2021). Briefly, recorded light is transmitted through fiber optical cables to a UV-VIS low stray light spectrometer (Herman et al., 2009; Tzortziou et al., 2012). The spectrometer covers a spectral range of 280-530 nm with a spectral resolution of 0.6 nm. To minimize the dark current noise, the spectrometer is maintained
105 at a stable temperature of 20°C with a thermoelectric cooler. The Pandora spectrometer operates in two daytime viewing geometries, namely, direct-sun (DS) and scattered sunlight or sky-scan (SS) (Figure 1), with varying degrees of temporal resolution spanning from milliseconds to minutes depending on the mode of operation.

The Pandora retrieval involves several sequential steps or data processing levels that are all
110 archived by PGN. Raw measurement spectra are archived as L0. L1 data include corrections for instrumental characteristics such as dark signal, non-linearity, latency, flat field, temperature sensitivity, stray light, and wavelength corrections. L2Fit data includes spectral fitting, which leads to slant column amount calculations relative to the reference spectrum employing DOAS analysis (Herman et al., 2009; Cede, 2022; Gebetsberger et al., 2023a). L2 data results from the conversion
115 from slant columns to vertical columns, lower tropospheric column amounts, surface concentrations, and profiles utilizing geometrical AMFs for direct sun and analytical methods for sky scan, briefly described in the supplement to this paper (section S1.1). The reported accuracy of the DS total vertical column of NO₂ is 2.7×10^{15} molecules cm⁻² (0.1 Dobson unit, where 1 DU = 2.7×10^{16} molecules cm⁻²) with a precision of 2.7×10^{14} molecules cm⁻² (0.01 DU) (Herman et al.,
120 2009). For HCHO DS a small statistical error up to 6% and notable systematic error up to 26% are reported (Spinei et al., 2018, 2021) while the recent Pandora Delrin-free instruments require more assessment for quantifying accuracy and precision. The Pandora SS measurements still lack a robust validation; however, the CINDI-2 intercomparison included a Pandora (named as NASA



instrument) and reported a bias for measurements in the SS mode of about -0.05×10^{16} molecules
125 cm^{-2} for HCHO column and about -0.02×10^{16} molecules cm^{-2} for NO_2 column against the median
of the participating instruments (Tirpitz et al., 2021; Verhoelst et al., 2021). A brief review on
current Pandora software and hardware changes, retrieval scheme, and data quality flagging are
discussed in supplementary section S1.1.



130 **Figure 1.** Block diagram of a Pandora instrument and its two viewing geometries.

2.2 Pandora observational schedule

Pandora instruments are locally operated and mainly run on the standard schedule alternating
135 between DS and SS mode, although there is an option for user-defined schedules. The DS and SS
modes also alternate between an Open (unfiltered) mode for NO_2 and a U340 (filtered for
maximum transmission near 340nm) mode for HCHO observations (Cede et al., 2021; Spinei et
al., 2018). A typical example of the Pandora standard schedule on a clear sky day is shown in
Figure 2a, with the typical total hours per day for each routine annotated. Typically, Pandora
140 spends about 1.5 hrs each day in DS NO_2 (SQ) and DS HCHO (SS, not to be confused with “sky-



scan”) modes and about 1.5 hrs each in SS mode for lower tropospheric columns of NO₂ and HCHO (EO) and HCHO only (EU). Longer more detailed sky scanning (EL and EK) occurs for a total of about 1-2 hrs for profile observations. Find Sun (FS) routines occur throughout the day, but only take a short time (few seconds) over each hour. Typically, Pandora spends 65% of the time in SS mode and 30% in DS mode under clear sky conditions. Further details of all Pandora routine acronyms are described in supplementary section S1.2 and the Pandora user manual (Cede et al., 2021). The total hours per day for each routine is annotated in Figure 2a. The inset panels in Figure 2 (b and c) provide a closer view of the schedule for an 18-minute window as the instrument switches between DS and SS modes. The varying effective measurement times (t_{eff}) illustrate the observation frequency for each mode and product. Generally, the Pandora instrument possesses the capability to capture solar spectra at adjustable integration times, ranging from 2.5 ms to 4 s, with an overall measurement duration of approximately 40 s, encompassing a few dark current measurements (Cede et al., 2021). The integration time for DS NO₂ (with no filter) under bright sun is about 4 ms, and roughly 4000 spectra are acquired repeatedly and averaged to obtain very high signal-to-noise ratios with high precision (Herman et al., 2018). For DS HCHO (with U340 filter), a longer integration time (30-1000 ms) is used; hence, there are fewer measurements for HCHO compared to NO₂. Typically, in the DS mode, there are about 5 times more observations of NO₂ compared to HCHO column per scan (Figure 2c). In the SS mode, zenith measurement scans are routinely collected at a specified azimuth angle, with the north or 0° being the preferred direction. The zenith angles scans can vary by site with the lowest scan typically occurring between 89° and 85° depending on viewing conditions available at the site. The extended SS measurements are taken at multiple zenith angles (section S1.2) to derive lower tropospheric columns and profiles typically up to 2-4 km.

165

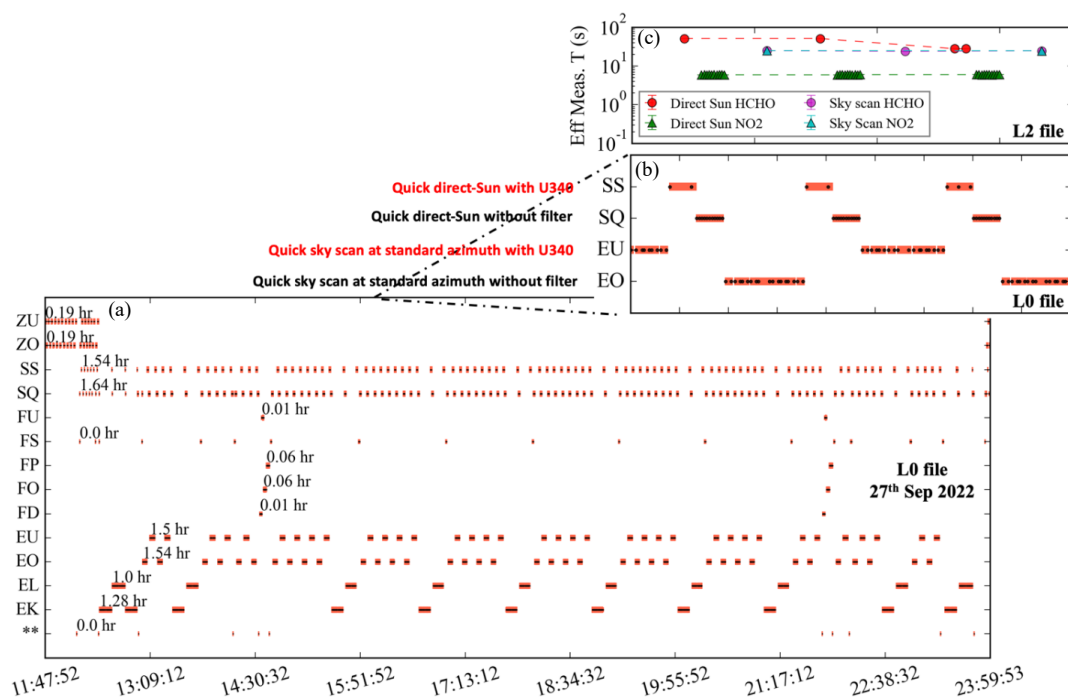


Figure 2. (a) Pandora standard schedule of operations (UTC hour) on a clear sky day on 27 Sep 2022 at the University of Houston site for different observing modes with a zoomed-in, 18-minute window for both L0 (b) and L2 (c) file information. The black points in the L0 schedule show the start of each measurement time and underlying red line is the total time in that respective mode. The L2 data (c) shows the alternating retrieval of NO₂ (without filter) and HCHO (with U340 filter) column from direct-sun and sky-scan modes.

3.0 Pandora data quality flags and an alternative data filtering method

The PGN team developed a software suite to perform retrievals for NO₂ and HCHO and provide a measure of data quality to guide users (Cede et al., 2021, 2023). Reduced data quality can arise from instrumental and/or atmospheric sources. Data flags provide information on both the data quality and data assurance level (Gebetsberger et al., 2023b). Data quality is indicated in the unit position, with a 0, 1, or 2 indicating high, medium, and low quality respectively. While data that is preliminary, but not yet quality assured, is useable for science, this status is indicated by a 1 in the tens position. Data that is unusable for whatever reason are indicated by a 2 in the tens position. Thus, data flagged as 0 or 10 are considered useable and high quality, and users are cautioned to pay additional scrutiny to data flagged as 1 or 11 (medium quality). By contrast, users are



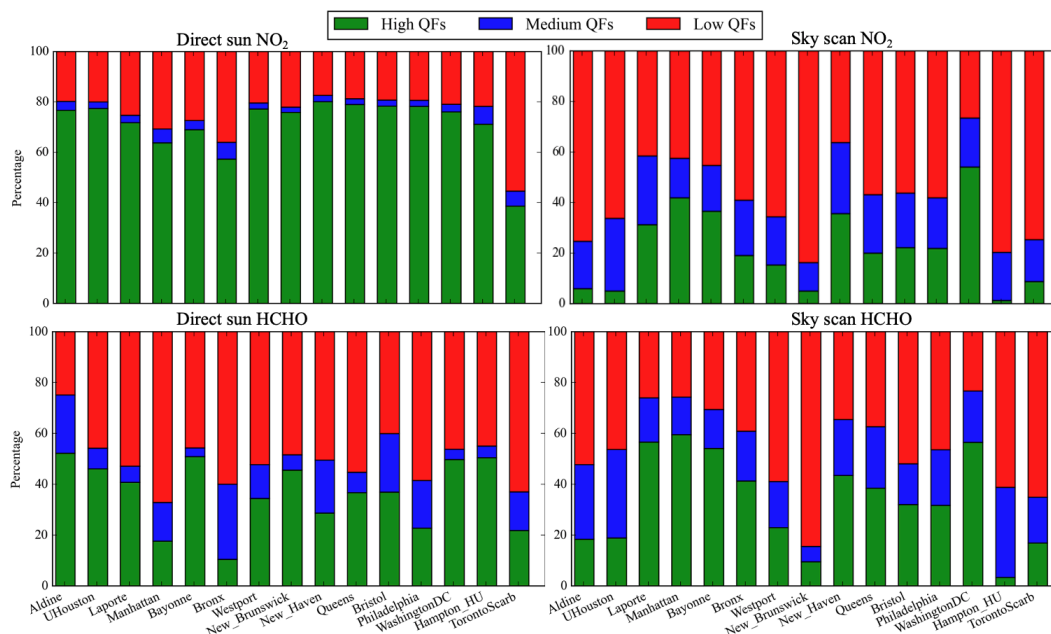
185 discouraged from using any data flagged as 2 or 12 (low quality). These quality flags are based on
threshold values of various parameters, i.e., uncertainties, wrms (normalized rms of the fitting
residuals weighted with the independent uncertainty), atmospheric variability (a measure of
radiance variance in field of view or measure of cloudiness), wavelength shift, and AMF (Table
S1). More description of the data quality flags is provided in supplementary section S1.1.

190 Following the suggestion of the Pandora user manual (Cede et al., 2021, 2023), many previous
studies with Pandora v1.8 data utilize only high-quality flag data (0, 10) (e.g., Park et al., 2022;
Verhoelst et al., 2021; Liu et al., 2023). However, when using only high-quality flagged data, a
large fraction of observations is often eliminated. Figure 3 shows quality flag statistics across the
15 Pandora sites evaluated in this study (listed in Table S2). They have been selected since they
195 fall under recent NASA airborne campaigns that covered areas of the eastern U.S and Houston,
TX. These are the Tracking Aerosol Convection Interactions Experiment-Air Quality (TRACER-
AQ) in 2021, the Student Airborne Research Program (SARP-East) in 2023, and the Synergistic
TEMPO Air Quality Science (STAQS) study in 2023. Across these sites, high-quality data flags
dominate only for DS NO₂ observations during the 2021-2022 period, typically being between 60-
200 80%. For other observations, low quality data flags often dominate, on average accounting for
57%, 45%, and 46% of data for SS NO₂, DS HCHO, and SS HCHO, respectively, across the
evaluated sites, making much of the data unavailable for supporting field campaign analysis.

The schedule of Pandora operations shown in Figure 2 demonstrates the contemporaneous nature
of DS and SS observations. Figure 3 further shows that the quality flags for the two observing
205 methods can often differ substantially. This enables an independent assessment of data quality by
looking at the correlation of contemporaneous (within 5 min) DS and SS observations for different
quality flag combinations. An example is provided in Figure 4 showing HCHO observations for
the University of Houston Pandora site. Note that there are nine possible combinations of high,
medium, and low-quality data pairs. More than half of those data pairs (57%) include one low-
quality observation. Low-quality SS observations correlate as well or better with medium and
210 high-quality data as do data pairings including only medium and high-quality data. There is more
scatter in the data that include low-quality DS observations (right column of panels in Figure 4),
but there is still evidence of a large number of well correlated data, even for pairings of low-quality



215 data for both DS and SS modes. Given the independent nature of the DS and SS observations, it is worthwhile to examine the role of measurement uncertainty in these correlations.



220 **Figure 3.** Percentage contribution of high (0, 10), medium (1, 11), and low (2, 12) quality flags for 15 Pandora sites for observations in both DS (left panels) and SS (right panels) modes during 2021-2022. Percentage contributions are shown for NO₂ in the top panels and HCHO in the bottom panels.

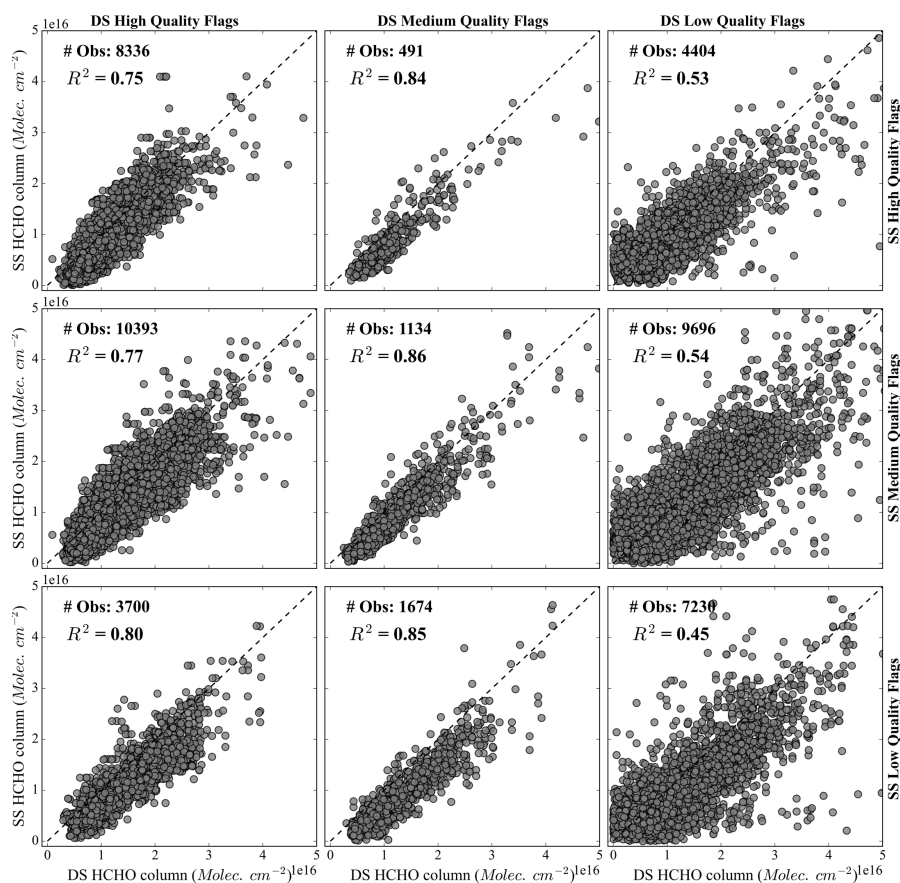
Figure 5 shows the frequency distribution of the retrieved independent uncertainty for high, medium, and low-quality Pandora HCHO and NO₂ column observations for both DS and SS mode for non-negative vertical columns at the University of Houston Pandora site. Independent uncertainty is a measure of the photon noise across the detector pixels which is propagated to slant columns for each retrieval and provided in the L2 product (Table S1). Figure 5 shows that there is significant overlap in the independent uncertainty distribution across all three quality flags for each measurement mode. The figure inset shows the corresponding cumulative probability distributions and a cut-off value (black dotted line) that preserves the high-quality data while including a significant amount of overlapping data flagged as medium or low quality. In the present analysis, the cut-off value for independent uncertainty is defined as $\mu + 3\sigma$ of the independent uncertainty distribution for high-quality data, where μ is mean and σ is standard deviation. The gray shaded

225

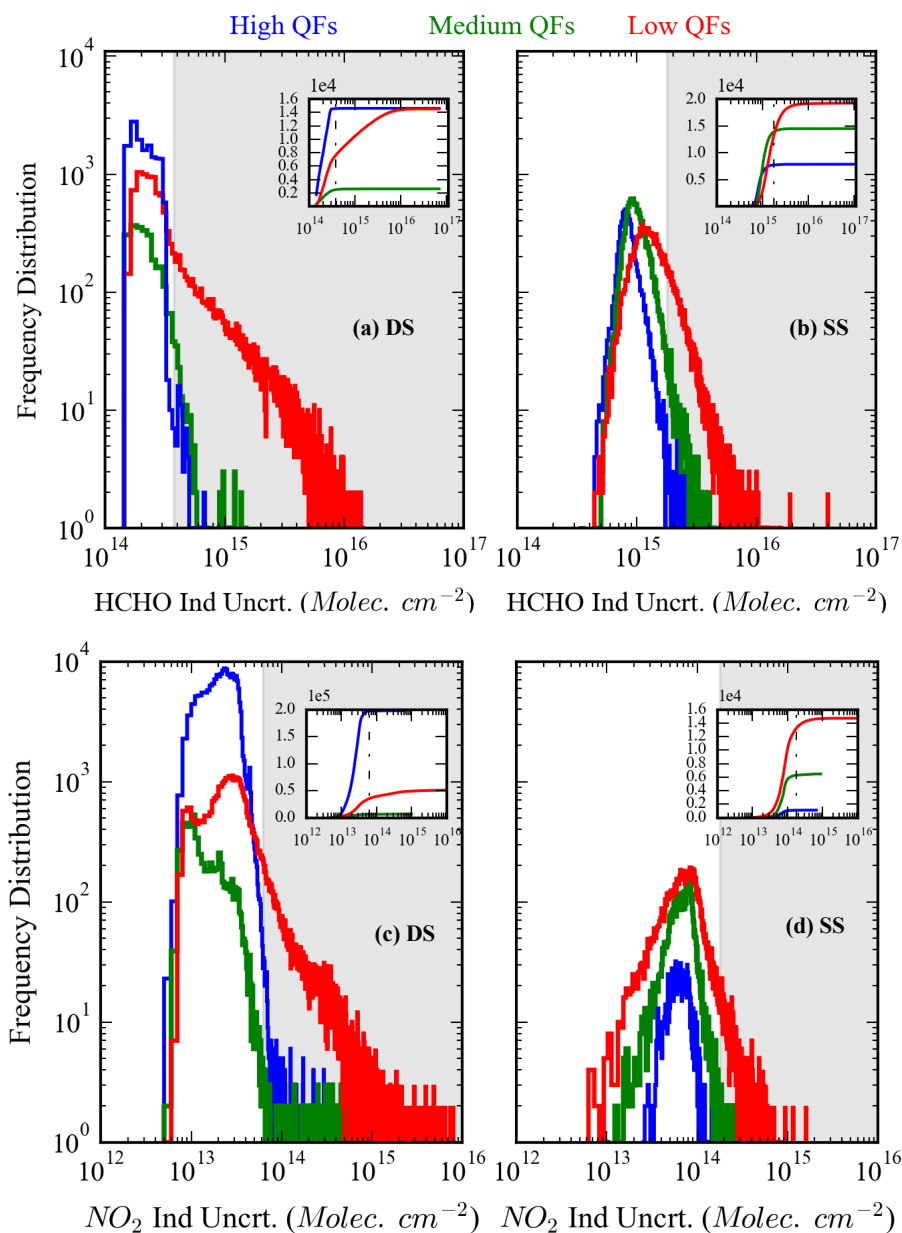
230



area in Figure 5 shows the portion of the data falling outside this limit. For the University of Houston Pandora, the cut-off values are 0.37×10^{15} molecules cm^{-2} for DS independent uncertainty and 1.79×10^{15} molecules cm^{-2} for SS independent uncertainty in HCHO column measurements. For NO_2 column measurements the cut-off values are 0.62×10^{14} molecules cm^{-2} for DS independent uncertainty and 1.81×10^{14} molecules cm^{-2} for SS independent uncertainty. In this method, Pandora data having independent uncertainty less than the cut-off limit are considered scientifically useful regardless of their data flag.



240 **Figure 4.** Correlation of contemporaneous DS and SS observations of HCHO column for different quality flag combinations. Data is from the University of Houston Pandora site over two years (2021-2022).



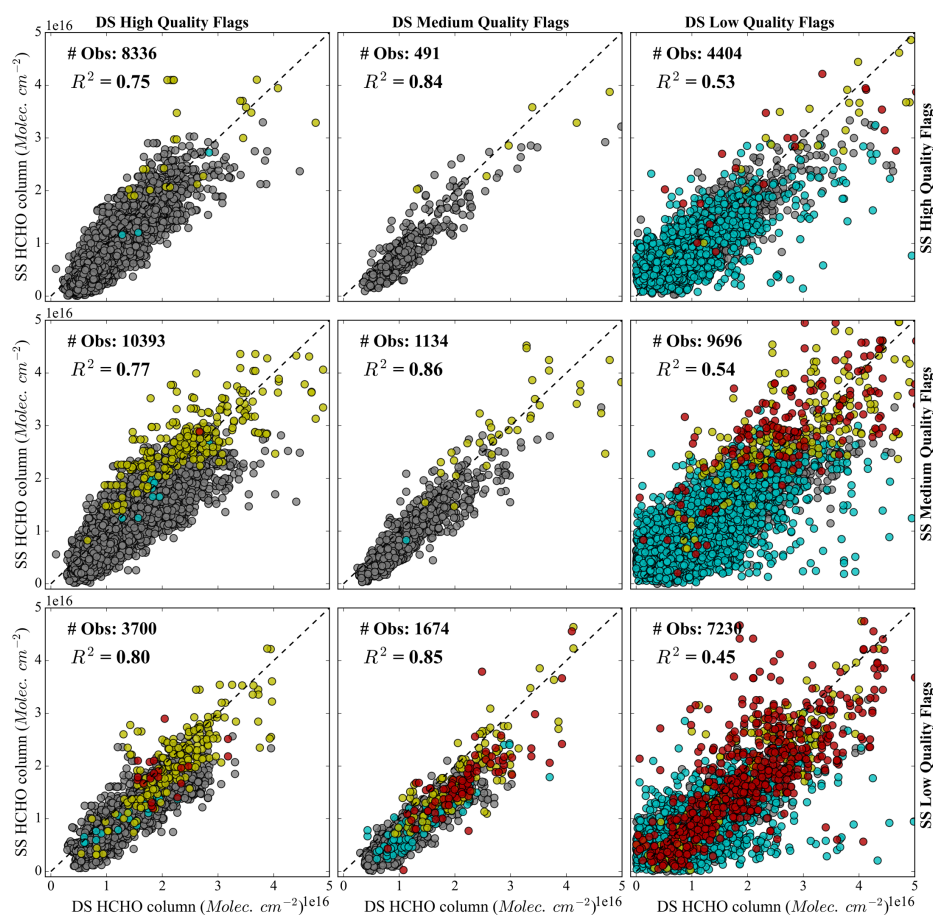
245 **Figure 5.** Frequency distribution of independent uncertainty in three quality flags: high (blue),
 medium (green) and low (red) for a) column HCHO direct-sun, b) column HCHO sky-scan, c)
 column NO₂ direct-sun, and d) column NO₂ sky-scan observations at the University of Houston
 Pandora site. The cumulative distributions for each panel are inset with the cut-off values used in
 the present analysis shown as a black dashed vertical line. Data values exceeding the cut-off are
 250 shaded in gray for the frequency distributions.



This proposed data filtering method is evaluated in Figure 6 for HCHO observations at the University of Houston Pandora site, showing how specific data pairs are related to the independent uncertainty cut-off values. Data pairs with uncertainty falling above the cut-off for DS only (blue points) and both DS and SS (red) are almost exclusively limited to the low-quality flagged data (right column and bottom row of panels in Figure 6). These points also account for most of the scatter in the correlations. Data pairs with uncertainty falling above the cut-off for SS data only (yellow) tend toward larger column amounts. This calls for a second filtering step in which observations with percent independent uncertainties of less than 10% of the column amount are retained even if the absolute independent uncertainty exceeds the cut-off value. This preserves a small but important set of large column abundances that are important for exploring the full dynamic range of column variability.

Finally, there can be a few rare outliers associated with unusually large wrms values even after applying this independent uncertainty cut-off. For this analysis, the additional handful of points with $wrms > 0.01$ are removed. Another variable specific to the SS observations is the maximum horizontal distance (MHZD) which can occasionally reach large values. For this analysis, data with $MHZD > 20$ km are removed as well. Specific column numbers from Pandora files for the variables used in this analysis are provided in Table S1 to facilitate application of this method.

Figure 7 shows the filtered data for the University of Houston Pandora site colored by data density. After the filtering method is applied, correlations notably improve for combinations that include DS low quality flagged data. Among all pairings ($R^2 = 0.72$ to 0.86), data quality flags no longer appear to be a useful predictor of correlation between contemporaneous SS and DS observations. This suggests that all remaining data may be scientifically useful regardless of quality flag. Figure 7 also shows that there is a bias between SS and DS observations for HCHO column. This is not unexpected given that SS observations are limited to the lower troposphere, but as discussed later in section 3.3, this bias must be addressed for applications where it is advantageous to combine SS and DS observations into a larger unified data set.



280

285

Figure 6. Correlation of contemporaneous DS and SS observations of HCHO column for different quality flag combinations at the University of Houston Pandora site over two years (2021-2022). Data points are colored by cutoff values used for HCHO column independent uncertainty values. Gray indicates points for which both DS and SS uncertainties are less than the cut-off, other colors indicate points for which only DS (cyan), only the SS (yellow), or both DS and SS (red) uncertainties exceed the cut-off value.

290

Figure 8 shows the same plot as Figure 6 but for NO₂ columns at the University of Houston Pandora site. There are more total pairs in this comparison since DS NO₂ observations are more frequent than HCHO (see Figure 2). Again, reasonable correlation is observed in all the quality flags ($R^2 = 0.68$ to 0.73). For NO₂, the filtering method leads to very little data being removed, thus correlations are essentially unchanged in Figure 9 for the filtered data. Again, there is a bias



with DS values being greater than SS values. This is mainly due to stratospheric NO₂ which is only detected in the DS mode (see discussion in section 3.3).

295

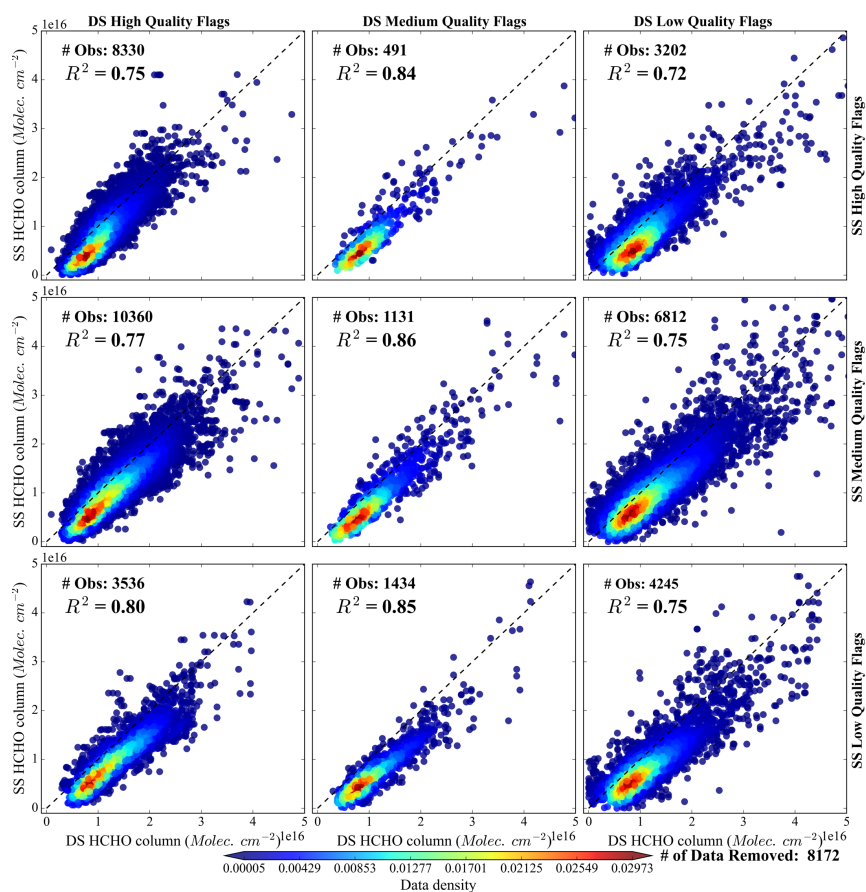


Figure 7. Correlation of contemporaneous DS and SS observations of HCHO column for different quality flag combinations after applying new filtering method to the University of Houston Pandora site for 2021-2022. Data points are colored by normalized gaussian kernel density of data.

300

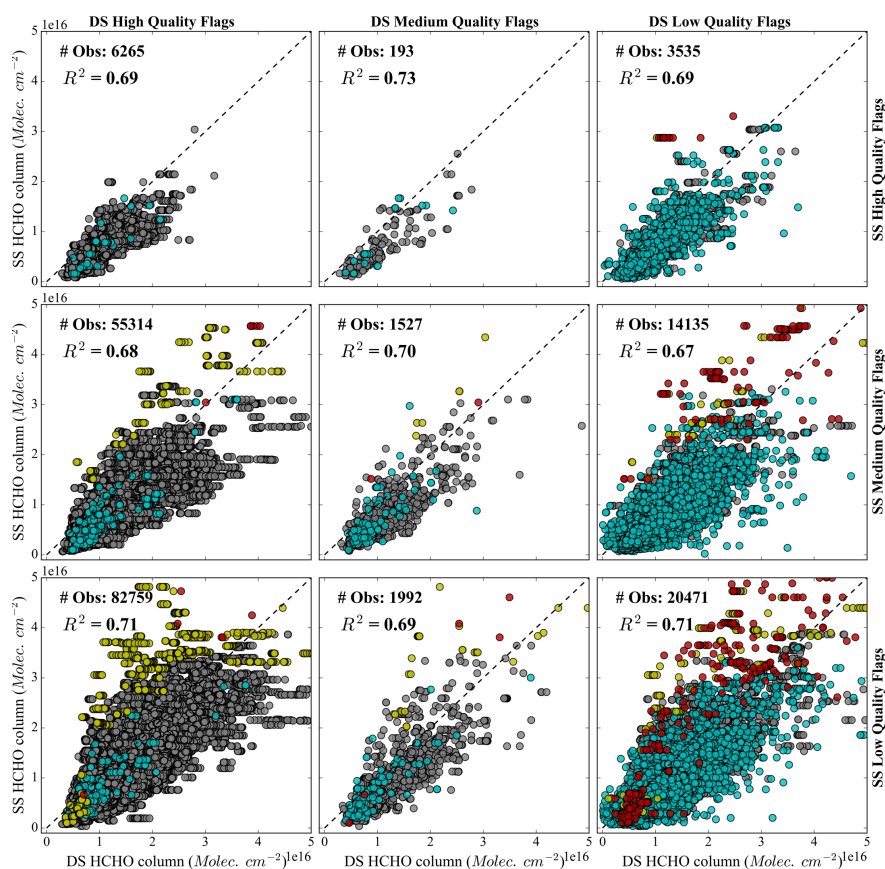
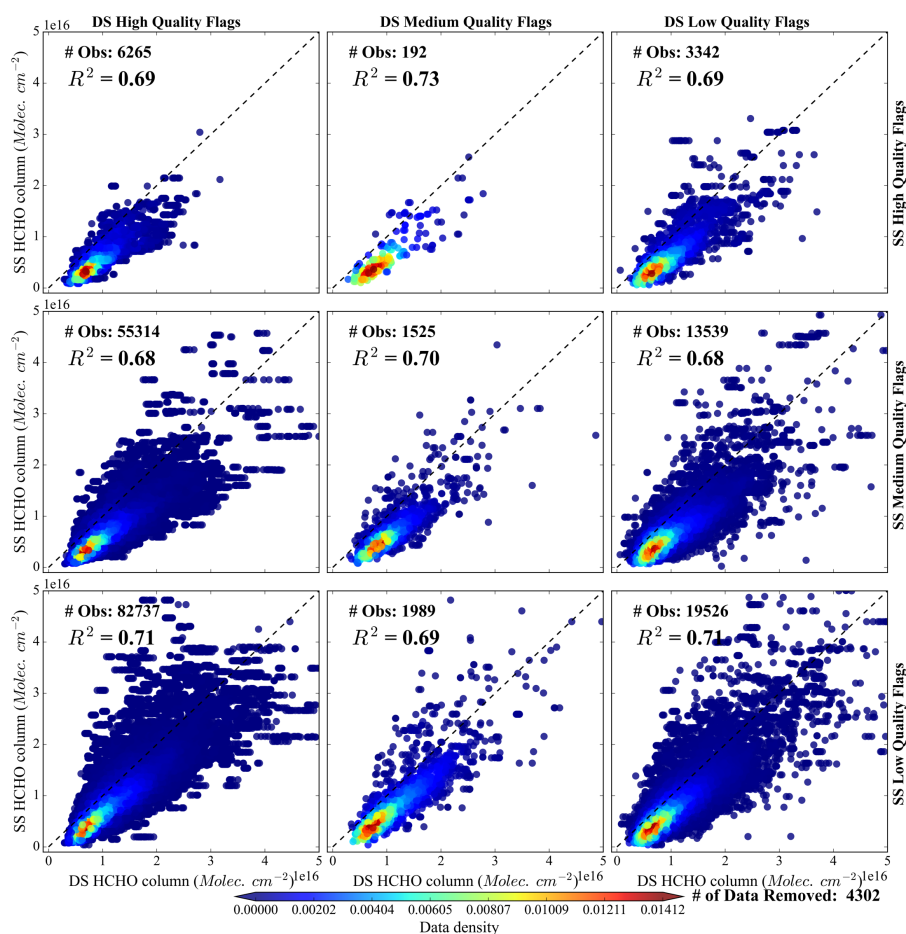
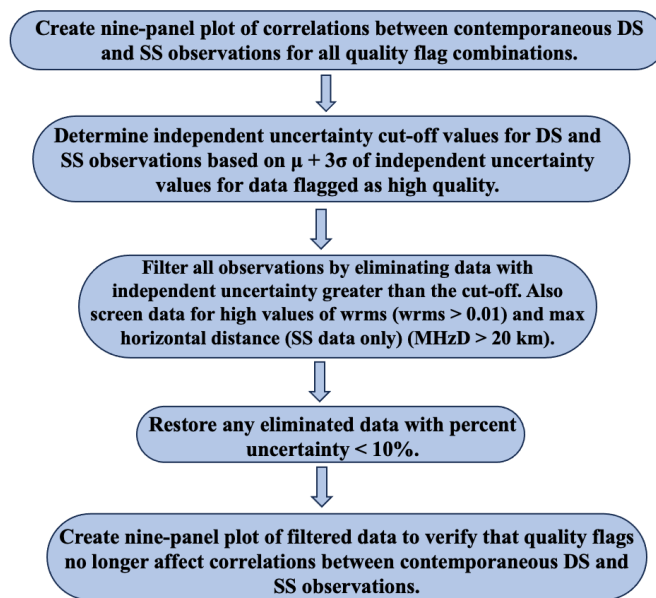


Figure 8. Correlation of contemporaneous DS and SS observations of NO_2 column for different quality flag combinations at the University of Houston Pandora site for 2021 – 2022. Data points are colored by cutoff values used for NO_2 column independent uncertainty values. Gray indicates points for which both DS and SS uncertainties are less than the cut-off, other colors indicate points for which only DS (cyan), only the SS (yellow), or both DS and SS (red) uncertainties exceed the cut-off value.

305



310 **Figure 9.** Correlation of contemporaneous DS and SS observations of NO_2 column for different quality flag combinations after applying new filtering method to the University of Houston Pandora site for 2021-2022. Data points are colored by normalized gaussian kernel density of data.



315 **Figure 10.** New data filtering method used in the present analysis to increase the scientific availability of Pandora observations.

The method demonstrated in Figures 4 through 9 is summarized in Figure 10. It can be applied to any PGN site with contemporaneous DS and SS observations. Results of applying the method are show in Figure 11 for the 15 Pandora sites falling under recent NASA airborne campaigns. Data from 2021 and 2022 are used for all sites, although La Porte, Texas only has data after August 320 2021 to February 2022. The bars in Figure 11 show the occurrences of the high (green), medium (blue), and low (red) quality flagged data across these 15 Pandora sites. The adjacent grey bar shows the amount of usable data after applying the new filtering method. Compared to using only high-quality flagged data, the new filtering method increases available data up to 90% for the HCHO column in both SS and DS modes (Figures 11c and 11d) and for NO₂ in SS mode (Figure 325 11b). Most DS NO₂ columns were already flagged as high quality, but the new filtering method still increases available data by 20% to 60% (Figure 11a). The amount of available data varies considerably between sites. This can be due to a number of reasons including instrument down time, use of non-standard observing schedules, and periods of data flagged as unusable (20, 21, or 22).

330



As noted in Figure 10, the first step in verifying the success of the method is to demonstrate the quality of correlation across all quality flag combinations. To further strengthen the case for using this method, independent observations are used in the following sections to demonstrate more robust scientific analyses. Evaluation of biases between DS and SS observations and prospects for combining them into a single data set are also explored.

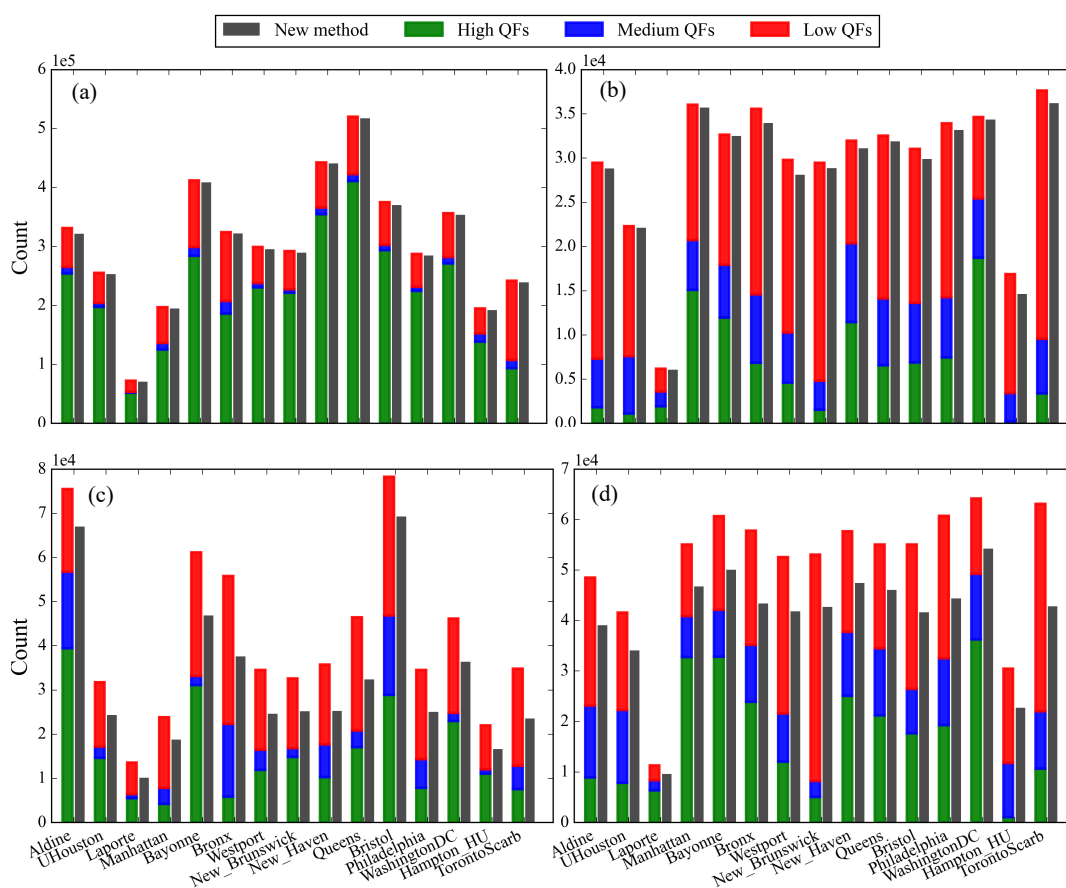


Figure 11. Quality flags (QFs) for each Pandora site in 2021-2022 (left bars) colored by green (high), blue (medium), and red (low) for (a) NO₂ DS, (b) NO₂ SS, (c) HCHO DS, and (d) HCHO SS. Adjacent grey bars show total observation counts after applying the new filtering method.



3.1 Independent assessment of Pandora scientific data quality with HCHO:O₃ analysis

345 Recent work has shown a strong correlation between surface O₃ and column HCHO (Schroeder et al., 2016; Travis et al., 2022). This relationship is used here to test the effectiveness of the new filtering method on Pandora HCHO column observations for the University of Houston Pandora site during the TRACER-AQ period (September 2021). High-resolution (5-min) collocated surface ozone measurements were obtained from the Texas Commission on Environmental Quality. The
350 Pandora HCHO column measurements in SS and DS modes are temporally matched (within 5 minutes) with surface ozone data between 10:00 and 18:00 local time when photochemistry is most active. This analysis compares results using only high-quality flagged Pandora data with results using Pandora data filtered with the new method.

355 Figure 12 shows the relationship between the HCHO column and surface ozone using DS and SS observations. When the new filtering method is applied, the R² substantially increased in SS mode from 0.42 (Figure 12a) to 0.57 (Figure 12c) with a five-fold increase in the number of data points (181 to 955). In DS mode, R² remained the same (Figure 12b and 12d) but with over a two-fold increase in data (275 to 696). Similar improvements in correlation and data quantity are obtained
360 for other months outside the TRACER-AQ period that are not shown here.

This analysis is expanded in Table 1 to include Pandora sites that are located within 500 m of an EPA regulatory monitor reporting hourly ozone. Data is for the month of September 2022 which had the best data availability. Table 1 summarizes the resulting correlation between hourly
365 averaged column HCHO in SS and DS modes with hourly surface ozone. Generally, similar or improved correlation and increased data availability (14 – 163%) were observed after applying the new filtering method. However, over the New Brunswick site in DS mode, a lower correlation (0.60 to 0.52) was observed after applying the new method. This was caused by the new method capturing an ozone event (>60 ppb) that appeared to be decoupled from high HCHO columns on
370 September 19, 2022. This independent analysis shows that recovered data can both improve the analysis of the HCHO:O₃ relationship and provide confidence in the scientific value of the new filtered dataset.



375

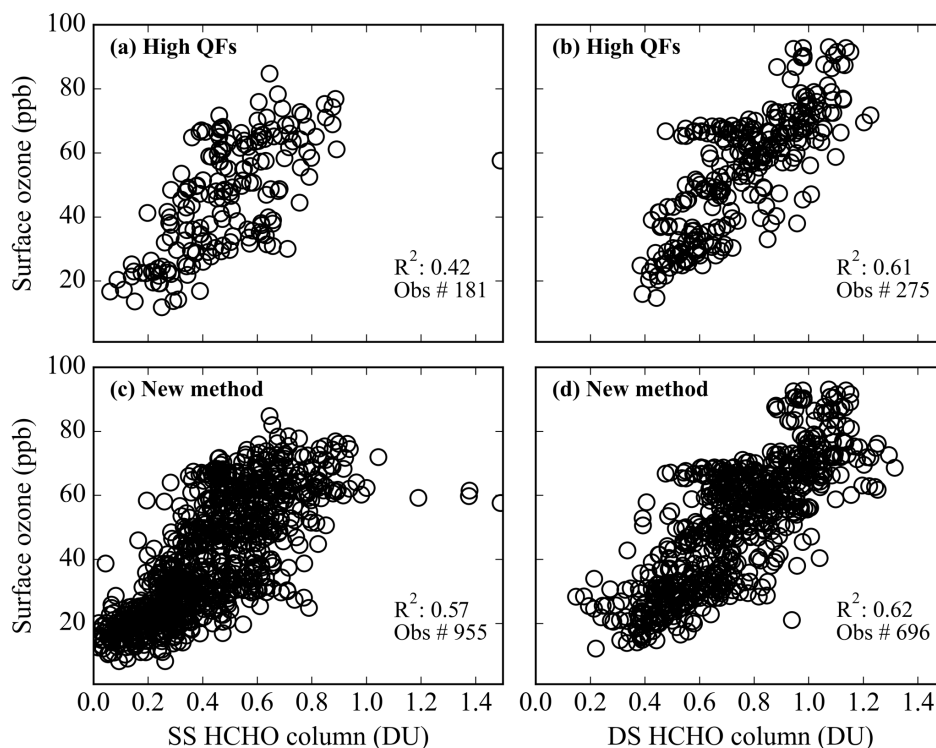


Figure 12. Relationship between Pandora HCHO column and surface ozone observations at the University of Houston site during TRACER-AQ in September 2021. Scatter plot between sky-scan HCHO column and surface ozone for (a) only high-quality flags and (c) data with new filtering method. Scatter plot between direct-sun HCHO column and surface ozone for (b) only high-quality flags and (d) data with new filtering method. HCHO column is given in Dobson units (1 DU = 2.69×10^{16} molecules cm^{-2}).

385

390



Table 1. Correlation (R^2) between hourly surface ozone and HCHO observations from direct sun and Sky scan for high-quality data flags alone and for data using the new filtering method. Analysis is for four Pandora sites during September 2022. Each site is located near (within 500 m) an ozone monitoring instrument. The number (n) is the available hourly matchups for each site.

Site	Direct-sun		Sky-scan	
	High Quality Flags	New Filtering Method	High Quality Flags	New Filtering Method
Manhattan	$R^2=0.36$, n=59	$R^2=0.43$, n=156	$R^2=0.62$, n=152	$R^2=0.64$, n=164
Westport	$R^2=0.47$, n=99	$R^2=0.55$, n=165	$R^2=0.56$, n=115	$R^2=0.57$, n=189
New Brunswick	$R^2=0.60$, n=154	$R^2=0.52$, n=211	$R^2=0.61$, n=222	$R^2=0.63$, n=246
Bristol	$R^2=0.71$, n=109	$R^2=0.67$, n=209	$R^2=0.74$, n=183	$R^2=0.72$, n=241

3.2 Independent assessment of Pandora scientific data quality with airborne remote sensing

GEO-CAPE airborne simulator (GCAS) observations (Nowlan et al., 2018; Judd et al., 2020) provide an independent dataset of column NO_2 and HCHO observations to compare against Pandora over Houston, TX during the TRACER-AQ period (September 2021). Looking downward as it flies overhead at ~ 8.5 km, GCAS measures a partial column from the aircraft altitude down to the surface that includes the polluted boundary layer and a large portion of the less polluted free troposphere. Figure 13 shows the comparison of DS and SS observations with GCAS NO_2 and HCHO. To minimize the temporal and spatial mismatch between the Pandora and GCAS observations, GCAS was spatially filtered to include the nearest cloud-free GCAS pixels within 2.5 km of the Pandora location, and Pandora was temporally filtered to include observations in a 15-minute window centered on the time of the GCAS overpass.

Both the DS and SS NO_2 columns are well-correlated with GCAS ($R^2 = 0.78$ and 0.64 , respectively). Some scatter can be attributed to GCAS uncertainties being on the order of 25% (Judd et al., 2020; Nawaz et al., 2024) from a priori uncertainties related to surface reflectivity and trace gas profile. For DS NO_2 columns, there is a clear offset with Pandora columns exceeding GCAS values. The slope near unity and intercept of 3×10^{15} molecules cm^{-2} is consistent with the stratospheric amount that would be absent in the GCAS observations below the aircraft. Despite a

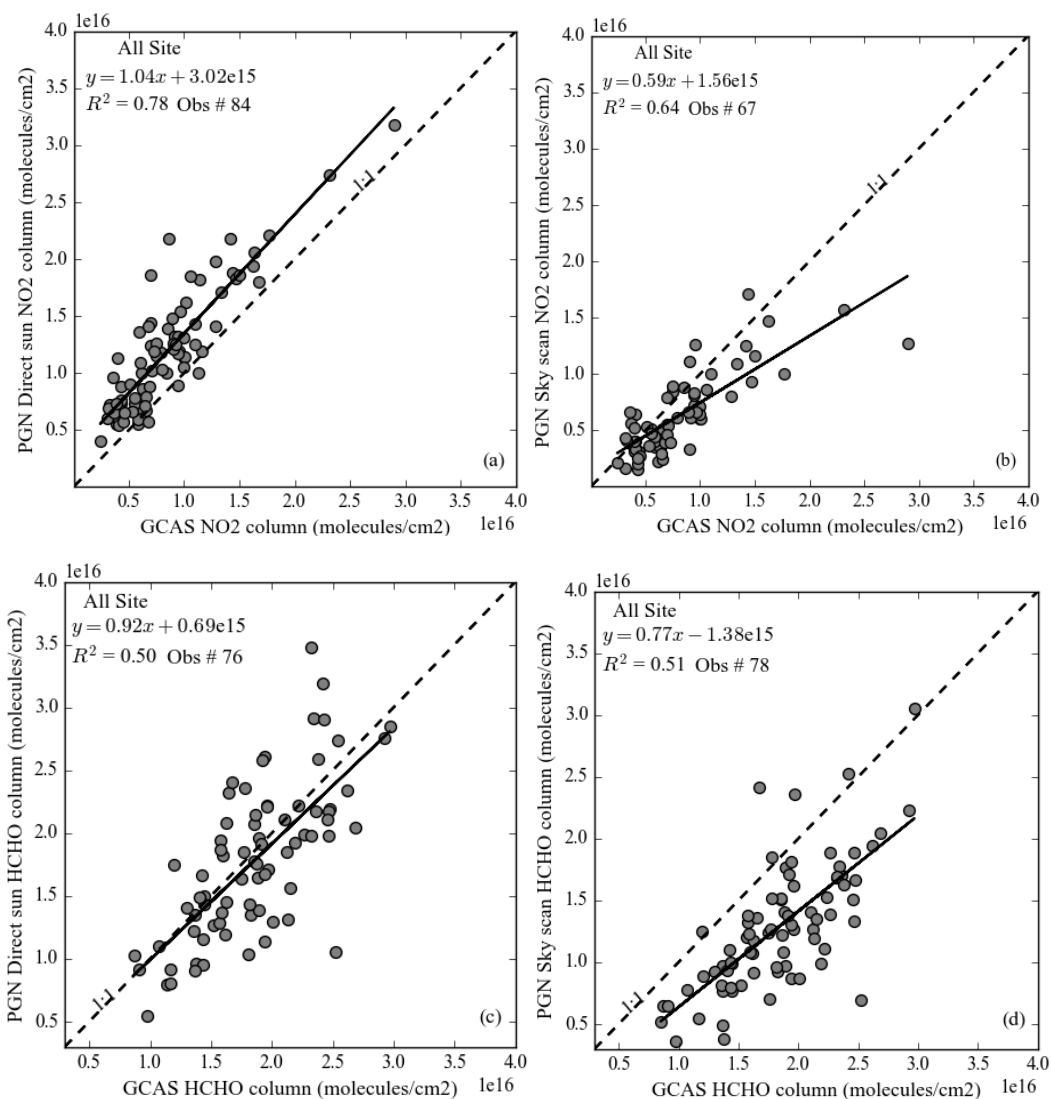


few outliers (Figure 11b), there is no notable systematic bias between GCAS and SS NO₂. This is consistent with the SS NO₂ observations being limited to the most polluted lower few kilometers of the atmosphere. It could be argued that GCAS values tend to be slightly higher than SS observations of NO₂ due to the larger altitude range observed.

420 The correlations for GCAS and Pandora HCHO columns also show general agreement ($R^2 = 0.50$
and 0.51) but are weaker primarily due to the greater uncertainty in HCHO measurements for both
instruments. For HCHO, the bias is in the SS rather than DS observations. This is due to the lack
of significant HCHO in the free troposphere and stratosphere; thus, total columns associated with
DS observations are more consistent with GCAS. Since HCHO is photochemically created, it tends
425 to have a weaker vertical gradient in the polluted boundary layer compared to NO₂ which is much
more weighted towards the surface where it is emitted. Thus, the limited altitude range of SS
observations are more likely to miss some fraction of lower atmospheric HCHO and be biased low
with respect to both DS and GCAS HCHO.

Overall, these comparisons are encouraging for both GCAS and Pandora with differences that are
430 consistent with expectations based on the differences in DS and SS viewing sensitivities.

435



440 **Figure 13.** Comparison of airborne GCAS trace gas columns with and Pandora columns of NO_2 (panels a and b) and HCHO (panels c and d) during TRACER-AQ for Houston Pandora sites (Aldine, La Porte, and University of Houston). Comparisons are shown for both direct-sun (panels a and c) and sky-scan (panels b and d) modes.



3.3 Direct-sun and sky-scan intercomparison of column amounts

Given that the Pandora instrument spends significant time in both DS and SS modes, maximum data availability for scientific applications would be achieved by further addressing the causes of differences in their resulting measurements. DS and SS column measurements are expected to differ in their absolute amount due to limitations in the vertical sensitivity (for SS measurements), retrieval method (Herman et al., 2009; Frieß et al., 2019), and physical differences between tropospheric and stratospheric amounts. SS columns generally profile from the surface up to 2-4 km while DS columns observe the total column through the entire atmosphere. Due to its short lifetime and major secondary source from chemistry, the HCHO column has a weak gradient from the surface through the depth of the boundary layer (Schroeder et al., 2016; Crawford et al., 2021). This suggests that the DS HCHO total column should be greater than the SS lower tropospheric column, and the difference should be largely dependent on the vertical sensitivity of the SS measurement, which most often ranges from the lowest 2-4 km of the atmosphere. For the NO₂ column, the stratospheric contribution is the largest influence on the differences between SS and DS column retrievals. To obtain a tropospheric DS NO₂ column, the NO₂ stratospheric column can be subtracted from the DS NO₂ total column using the stratospheric climatology provided by the PGN in their product based on Brohede et al., (2007).

Figure 14a shows the mean differences between the DS and SS column for HCHO and NO₂ over the 15 Pandora sites for 2021-2022. The bias for HCHO on average is 3.4×10^{15} molecules cm⁻² with a larger bias at Hampton University in Virginia and New Haven, Connecticut ($>5 \times 10^{15}$ molecules cm⁻²) and the smallest bias at Bayonne, New Jersey. The mean HCHO column in DS mode over these 15 sites averaged about 1×10^{16} molecules cm⁻² making the bias between DS and SS mode approximately 35% of the column.

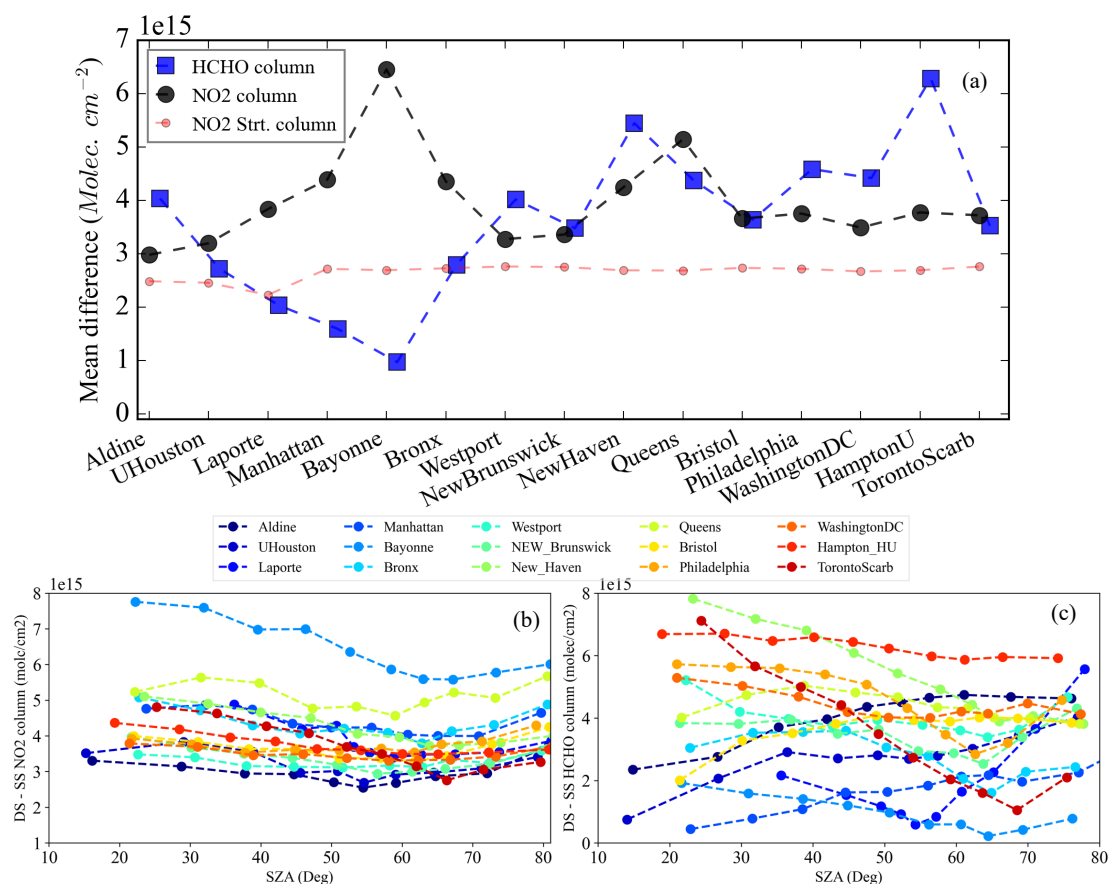
For NO₂, the mean difference was calculated after removing the stratospheric contribution (see red line in Figure 14a, Figure 14 is without removing stratospheric contribution). The remaining bias was less than 1×10^{15} or about 20% of the tropospheric column (5×10^{15}) on average. Higher average NO₂ columns ($>10 \times 10^{15}$ molecules cm⁻²) were observed in New York (Manhattan, Bronx, and Queens) which also had three of the four highest biases observed. The highest bias was at Bayonne and appears to be anomalous, demonstrating that bias comparisons across the network are a useful tool for identifying potential problems at specific sites. In this case, Bayonne's large bias in NO₂



between SS and DS deserves a closer look by the site operator and may be related to a reference spectrum or calibration issue.

Figure 14 also shows how the bias between DS and SS for NO₂ (b) and HCHO (c) changes with solar zenith angle (SZA). One reason to expect changes in the bias with SZA is the larger uncertainty in AMF calculations and larger stray light contribution at high SZA (Herman et al., 2009). However, no consistent patterns in bias behavior versus SZA was found for either HCHO or NO₂. Pandoras at Aldine and the University of Houston showed increasing biases with increasing SZA for HCHO but the bias decreases with SZA at New Haven and Toronto and showed no variations with SZA for the New York Pandora instruments. The NO₂ column biases as a function of SZA showed no notable variation and were mostly constant around a mean value. Additionally, stray light is minimized in Pandora DS retrievals by subtracting the average signal below 290 nm from the spectra and using other correction methods (Cede et al., 2021). However, residual stray light could contribute to large difference between DS and SS HCHO columns. Plotting the residual stray light as a function of SZA (Figure S1) showed that it decreased or remained constant (~ 0.3%) with increasing SZA, which suggests stray light contribution to the column might not increase significantly at higher SZA. There is also no evidence for a seasonal dependence in the difference between SS and DS observations (Figure S2 for the University of Houston), unlike that reported for the total ozone biases between Pandora and Brewer observations (Tzortziou et al., 2012).

Finally, the importance of differences in pointing azimuth and solar azimuth angle was investigated since 1) the Pandora SS analytical method may be less accurate when the solar azimuth and pointing azimuth are close (Cede et al., 2021), and 2) when the difference is large, the retrievals may be sampling different air masses. Figure S3 shows no systematic biases as a function of the difference between the pointing azimuth and solar azimuth across all 15 sites. This suggests that retrieval uncertainties and vertical sensitivity are most likely responsible for the mean biases between the SS and DS columns. This allows for the possibility of combining the two datasets for higher temporal coverage.



505

Figure 14. (a) Mean differences between the DS and SS column for HCHO and NO₂ over the 15 Pandora sites for 2021-2022. The NO₂ stratospheric column for each site is also provided. Bottom panels show the variation of mean column difference with SZA for NO₂ column (b) and HCHO columns (c), respectively.

510

3.4 Temporally combining DS and SS data

Section 2.2 discussed the standard schedule for Pandora observations with alternating measurements in the DS and SS modes and use of UV and open filters for the HCHO and NO₂ observations, respectively. The DS NO₂ retrieval is relatively fast compared to DS HCHO measurements which are less frequent. For SS measurements, both HCHO and NO₂ are comparable and take much longer than DS measurements (Figure 2c). In order to be combined, these time differences as well as biases diagnosed in the previous section must be addressed.

515



With the goal of creating a more continuous data record of hourly HCHO columns from Pandora suitable for comparison with hourly in situ measurements of surface ozone at EPA sites, Equation 1 combines data for DS and SS modes by correcting for the mean bias and then accounting for the difference in measurement times. Each column is weighted by the ratio between measurement time in each mode and total measurement time during the hour for both DS and SS modes. DS values for NO₂ column must first include subtraction of the stratospheric NO₂ contribution. SS observations are corrected by adding the mean bias value (Figure 14a). The summation of weighted values results in an hourly Pandora HCHO column.

$$X_{\text{combined}} = \sum_{i=1}^{1\text{hr}} X_{\text{DS}}[i] \times \frac{t_{\text{eff}}[i]}{\text{Tot}} + \sum_{j=1}^{1\text{hr}} \{X_{\text{SS}}[j] + \text{MB}\} \times \frac{\Delta t[j]}{\text{Tot}} \quad \text{Eq. 1}$$

where t_{eff} is the effective measurement time for each DS observation (see column 3: “Effective duration of measurement” in the Pandora data files), Δt is the estimated measurement time for each SS observation (see Section S1.2 for details), Tot is the total integrated measurement time in a 1-hour period for both DS and SS measurements, $X_{\text{DS}}[i]$ is direct-sun column and $X_{\text{SS}}[j]$ is sky-scan column for the i^{th} and j^{th} measurements of each hour, respectively. MB is the mean bias of HCHO and NO₂ column between DS and SS measurements.

Table 2 shows the performance of the relationship between HCHO and hourly surface ozone at the University of Houston during September 2021 for SS, DS, and the combined dataset. The hourly correlation remains similar compared to high resolution data (5 min) as discussed in Figure 12, however the number of observations is lesser. The combined data set with new filtering method increased the temporal coverage of Pandora observations on the hourly data compared to using only one mode and high-quality flagged data. Applying the new filtering method to the combined data results in the greatest data coverage with better or equivalent correlation than for other subsets of data.



545 **Table 2.** Correlation (R^2) between hourly surface ozone and column HCHO from Sky-scan, Direct-sun, and combined data at the University of Houston site during TRACER-AQ (Sept 2021). Results include data with high quality only and with the new filtering method. The number of analyzed hours (n) is given for each case.

HCHO:O ₃	High QFs	New filtering method
Sky-scan	$R^2=0.41$, n=132	$R^2=0.61$, n=234
Direct-sun	$R^2=0.59$, n=102	$R^2=0.58$, n=191
Combined data	$R^2=0.50$, n=162	$R^2=0.62$, n=240

550 4 Summary and conclusions

The growing Pandora Global Network of Pandora spectrometers provides a ground-based network of remote sensing observations to both validate satellite trace gas retrievals and understand local air quality. Pandora provides information on the diurnal variability of multiple species (e.g., NO₂ and HCHO) using two independent viewing geometries: direct-sun (DS) and sky-scan (SS) mode. The Pandora quality assurance procedure recommends using high-quality 555 flagged data, exercising caution with medium-quality flagged data, and not using low-quality flagged data. Unfortunately, high quality data can often be only a small fraction of the total set of observations, except for DS NO₂ columns.

This work presents a new filtering method developed and tested as an alternative to using quality 560 flags to identify scientifically useful observations. The method keys on the range of independent uncertainty values for Pandora data flagged as high quality. Given the large overlap in independent uncertainty for high-, medium-, and low-quality flagged data, the $\mu+3\sigma$ value of independent uncertainty for the high-quality flagged data defines a cut-off that preserves almost all high-quality data and includes a large amount of medium- and low-quality flagged data. For a much smaller 565 number of data, wrms > 0.001 (normalized root mean square of the fitting residuals weighted with



the independent uncertainty) and SS MHZD > 20 km (maximum horizontal distance) should also be filtered out. A final step in the method is to restore observations with a percent uncertainty of less than 10%.

570 Given the independence and contemporaneous nature of DS and SS observation modes, correlation
of adjacent (within 5 min) observations between modes provides evidence for scientifically useful
data in the medium- and low-quality flagged data. Unfiltered observations already exhibit some
degree of correlation for data with medium- and low-quality flags, but for filtered data, quality
flags appear to have no influence on correlations for various pairing of DS and SS quality flags.
This is particularly important in that the method can recover as much as 90% of data that would
575 have previously been discarded.

The strong relationship between column HCHO and surface ozone provided a method for testing
the new filtering method. At the University of Houston and four additional sites with nearby ozone
monitors, filtered data resulted in a similar or improved relationship between column HCHO and
surface ozone with 14-63% more data than using high quality data alone.

580 Airborne GCAS observations from the TRACER-AQ campaign in Houston provided an
independent set of NO₂ and HCHO column observations to compare against filtered Pandora DS
and SS observations. The two datasets correlated well, but biases were also observed related to
differences in the total column DS observations versus SS observations that have sensitivity
limited to the lowest 2-4 km of the atmosphere.

585 Combining SS and DS data provided better hourly data coverage after correcting for biases
between the two modes. Across 15 Pandora sites in the domain of recent NASA field campaigns,
the HCHO column biases ranged from 0.8×10^{15} molecules cm⁻² to 6×10^{15} molecules cm⁻² (8 to
60% of the average column of 1×10^{16} molecules cm⁻²). The NO₂ tropospheric column biases were
less than 1×10^{15} molecules cm⁻² (20% of the average column of 0.5×10^{16} molecules cm⁻² except
590 for at the Bayonne, NJ Pandora). The biases in NO₂ and HCHO between DS and SS observations
were examined for trends with solar zenith angle (SZA), viewing azimuth angle, and residual stray
light. No systematic behavior in the biases were found.



A more continuous hourly Pandora dataset was constructed for comparison with hourly surface ozone. This dataset required correcting the site-specific biases in DS and SS observations as well as weighting the observations based on their different measurement durations. The combined hourly dataset showed similar or improved correlations with surface ozone with a 30-40% increase in hourly data coverage.

The proposed filtering method and improved representation of hourly average conditions by combining DS and SS data offer the community useful strategies for using Pandora observations to their fullest potential for validating geostationary satellite observations and informing local air quality.

Data availability. The Pandora data is available at PGN website (<https://www.pandonia-global-network.org>). The airborne GCAS observation during TRACER-AQ period can be obtained from <https://www-air.larc.nasa.gov/cgi-bin/ArcView/traceraq.2021>. Surface ozone data at hourly and 5-minutes resolution is obtained from the EPA (<https://www.epa.gov/ground-level-ozone-pollution>) and ARM-TRACER-AQ (<https://adc.arm.gov/discovery/#/results/s::tracer%20tceq>) website, respectively.

Author contributions. PR, JHC, and KRT designed the study and PR performed the data analysis. PR and KRT interpreted the results and wrote the initial draft of the paper. LJ, JHC, KRT, JS, LV, MAGD, AW, EB and TFH provided significant conceptual input to the design of the manuscript and the improvement of the manuscript. All authors discussed the results and analysis.

Competing interests. At least one of the (co-)authors is a member of the editorial board of Atmospheric Measurement Techniques.

Acknowledgements. We thank the PI(s), support staff and funding for establishing and maintaining the 15 Pandora sites of the PGN used in this investigation, specifically we thank Jimmy Flynn, Maria Tzortziou, Nader Abuhassan, John Anderson, and Vitali Fioletov. We thank the ESA and NASA joint PGN for Pandora data processing and data disseminations. We thank NASA GFSC for Pandora calibration, in particular Apoorva Pandey and Bryan Place. NASA Postdoctoral Program at the NASA Langley Research Center, administered by ORAU under contract with NASA acknowledged for funding PR. LMJ and KRT acknowledge NASA grant



80NSSC24M0094. We acknowledge the GCAS groups for the TRACER-AQ 2021 filed campaign datasets. We thank EPA and TCEQ for surface ozone observations.

Disclaimer: The research described in this article has been reviewed by the U.S. Environmental Protection Agency (EPA) and approved for publication. Approval does not signify that the contents necessarily reflect the views and the policies of the agency nor does mention of trade names or commercial products constitute endorsement or recommendation for use.

References:

- Adams, T. J., Geddes, J. A., and Lind, E. S.: New Insights Into the Role of Atmospheric Transport and Mixing on Column and Surface Concentrations of NO₂ at a Coastal Urban Site, *JGR Atmospheres*, 128, e2022JD038237, <https://doi.org/10.1029/2022JD038237>, 2023.
- Brohede, S. M., Haley, C. S., McLinden, C. A., Sioris, C. E., Murtagh, D. P., Petelina, S. V., Llewellyn, E. J., Bazureau, A., Goutail, F., Randall, C. E., Lumpe, J. D., Taha, G., Thomasson, L. W., and Gordley, L. L.: Validation of Odin/OSIRIS stratospheric NO₂ profiles, *J. Geophys. Res.*, 112, 2006JD007586, <https://doi.org/10.1029/2006JD007586>, 2007.
- Cede, A., Herman, J., Richter, A., Krotkov, N., and Burrows, J.: Measurements of nitrogen dioxide total column amounts using a Brewer double spectrophotometer in direct Sun mode, *Journal of Geophysical Research: Atmospheres*, 111, <https://doi.org/10.1029/2005JD006585>, 2006.
- Cede, A., Tiefengraber, M., Gebetsberger, M., and Kreuter, M.: TN on Manual for Blick Software Suite 1.8, Pandonia Global Network, available at: https://www.pandonia-global-network.org/wp-content/uploads/2021/09/BlickSoftwareSuit_Manual_v1-8-4.pdf (last access: 27 Sep 2023), 2021.
- Cede, A., Santana, D., Tiefengraber, M., Muller, M., and Gebetsberger, M.: on Fiducial Reference Measurements for Air Quality, TN on change/upgrade of instrument, Pandonia Global Network, available at: https://www.pandoniaglobalnetwork.org/wpcontent/uploads/2022/12/LuftBlick_FRM4AQ_InstrumentChangeUpgrade_RP_2019002_v8.pdf (last access: 27 Sep 2023), 2022.
- Cede, A., Tiefengraber, M., Gebetsberger, M., and Lind E.: TN on Pandonia Global Network Data Products Readme Document version 1.8-7, Pandonia Global Network, available at: https://www.pandoniaglobalnetwork.org/wpcontent/uploads/2023/08/PGN_DataProducts_Readme_v1-8-7.pdf (last access: 27 Sep 2023), 2023.
- Chang, L.-S., Kim, D., Hong, H., Kim, D.-R., Yu, J.-A., Lee, K., Lee, H., Kim, D., Hong, J., Jo, H.-Y., and Kim, C.-H.: Evaluation of correlated Pandora column NO₂ and in situ surface NO₂



- 655 measurements during GMAP campaign, *Atmos. Chem. Phys.*, 22, 10703–10720, <https://doi.org/10.5194/acp-22-10703-2022>, 2022.
- Choi, S., Lamsal, L. N., Follette-Cook, M., Joiner, J., Krotkov, N. A., Swartz, W. H., Pickering, K. E., Loughner, C. P., Appel, W., Pfister, G., Saide, P. E., Cohen, R. C., Weinheimer, A. J., and Herman, J. R.: Assessment of NO₂ observations during DISCOVER-AQ and KORUS-AQ field campaigns, *Atmos. Meas. Tech.*, 13, 2523–2546, <https://doi.org/10.5194/amt-13-2523-2020>, 2020.
- 660 Crawford, J.H., Ahn, J.Y., Al-Saadi, J., Chang, L., Emmons, L.K., Kim, J., Lee, G., Park, J.H., Park, R.J., Woo, J.H. and Song, C.K., The Korea–United States air quality (KORUS-AQ) field study. *Elem Sci Anth*, 9(1), p.00163, 2021.
- 665 Di Bernardino, A., Mevi, G., Iannarelli, A. M., Falasca, S., Cede, A., Tiefengraber, M., and Casadio, S.: Temporal Variation of NO₂ and O₃ in Rome (Italy) from Pandora and In Situ Measurements, *Atmosphere*, 14, 594, <https://doi.org/10.3390/atmos14030594>, 2023.
- Frieß, U., Beirle, S., Alvarado Bonilla, L., Bösch, T., Friedrich, M. M., Hendrick, F., Pitters, A., Richter, A., Van Roozendaal, M., Rozanov, V. V., Spinei, E., Tirpitz, J.-L., Vlemmix, T., Wagner, T., and Wang, Y.: Intercomparison of MAX-DOAS vertical profile retrieval algorithms: studies using synthetic data, *Atmos. Meas. Tech.*, 12, 2155–2181, <https://doi.org/10.5194/amt-12-2155-2019>, 2019.
- Gebetsberger, M., and Tiefengraber, M.: on Evolution of QA/QC Strategies, Pandonia Global Network, available at: https://www.pandoniaglobalnetwork.org/wpcontent/uploads/2023/08/PGN_DataProducts_Readme_v1-8-7.pdf (last access: 27 Sep 2023), 2023a.
- 675 Gebetsberger, M., Tiefengraber, M., Cede, A.: Fiducial Reference Measurements for Air Quality, TN on Data Quality Flagging Generic Procedure Evolution, Pandonia Global Network, available at: https://www.pandoniaglobalnetwork.org/wpcontent/uploads/2023/08/PGN_DataProducts_Readme_v1-8-7.pdf (last access: 27 Sep 2023), 2023b.
- 680 Goldberg, D. L., Lamsal, L. N., Loughner, C. P., Swartz, W. H., Lu, Z., and Streets, D. G.: A high-resolution and observationally constrained OMI NO₂ satellite retrieval, *Atmos. Chem. Phys.*, 17, 11403–11421, <https://doi.org/10.5194/acp-17-11403-2017>, 2017.
- Herman, J., Cede, A., Spinei, E., Mount, G., Tzortziou, M., and Abuhassan, N.: NO₂ column amounts from ground-based Pandora and MFDOAS spectrometers using the direct-sun DOAS technique: Intercomparisons and application to OMI validation, *J. Geophys. Res.*, 114, D13307, <https://doi.org/10.1029/2009JD011848>, 2009.
- 685 Herman, J., Spinei, E., Fried, A., Kim, J., Kim, J., Kim, W., Cede, A., Abuhassan, N., and Segal-Rozenhaimer, M.: NO₂ and HCHO measurements in Korea from 2012 to 2016 from Pandora spectrometer instruments compared with OMI retrievals and with aircraft measurements during the KORUS-AQ campaign, *Atmos. Meas. Tech.*, 11, 4583–4603, <https://doi.org/10.5194/amt-11-4583-2018>, 2018.
- 690



- 695 Herman, J., Abuhassan, N., Kim, J., Kim, J., Dubey, M., Raponi, M., and Tzortziou, M.: Underestimation of column NO₂ amounts from the OMI satellite compared to diurnally varying ground-based retrievals from multiple PANDORA spectrometer instruments, *Atmos. Meas. Tech.*, 12, 5593–5612, <https://doi.org/10.5194/amt-12-5593-2019>, 2019.
- Ialongo, I., Virta, H., Eskes, H., Hovila, J., and Douros, J.: Comparison of TROPOMI/Sentinel-5 Precursor NO₂ observations with ground-based measurements in Helsinki, *Atmos. Meas. Tech.*, 13, 205–218, <https://doi.org/10.5194/amt-13-205-2020>, 2020.
- 700 Judd, L. M., Al-Saadi, J. A., Valin, L. C., Pierce, R. B., Yang, K., Janz, S. J., Kowalewski, M. G., Szykman, J. J., Tiefengraber, M., and Mueller, M.: The Dawn of Geostationary Air Quality Monitoring: Case Studies From Seoul and Los Angeles, *Front. Environ. Sci.*, 6, 85, <https://doi.org/10.3389/fenvs.2018.00085>, 2018.
- 705 Judd, L. M., Al-Saadi, J. A., Janz, S. J., Kowalewski, M. G., Pierce, R. B., Szykman, J. J., Valin, L. C., Swap, R., Cede, A., Mueller, M., Tiefengraber, M., Abuhassan, N., and Williams, D.: Evaluating the impact of spatial resolution on tropospheric NO₂ column comparisons within urban areas using high-resolution airborne data, *Atmos. Meas. Tech.*, 12, 6091–6111, <https://doi.org/10.5194/amt-12-6091-2019>, 2019.
- 710 Judd, L. M., Al-Saadi, J. A., Szykman, J. J., Valin, L. C., Janz, S. J., Kowalewski, M. G., Eskes, H. J., Veefkind, J. P., Cede, A., Mueller, M., Gebetsberger, M., Swap, R., Pierce, R. B., Nowlan, C. R., Abad, G. G., Nehrir, A., and Williams, D.: Evaluating Sentinel-5P TROPOMI tropospheric NO₂ column densities with airborne and Pandora spectrometers near New York City and Long Island Sound, *Atmos. Meas. Tech.*, 13, 6113–6140, <https://doi.org/10.5194/amt-13-6113-2020>, 2020.
- 715 Kim, J., Kim, M., and Choi, M.: Monitoring aerosol properties in east asia from geostationary orbit: GOCI, MI and GEMS, in *Air Pollution in Eastern Asia: An Integrated Perspective ISSI Scientific Report Series*. (Cham: Springer), 323–333, 2017.
- 720 Kim, S., Kim, D., Hong, H., Chang, L.-S., Lee, H., Kim, D.-R., Kim, D., Yu, J.-A., Lee, D., Jeong, U., Song, C.-K., Kim, S.-W., Park, S. S., Kim, J., Hanisco, T. F., Park, J., Choi, W., and Lee, K.: First-time comparison between NO₂ vertical columns from Geostationary Environmental Monitoring Spectrometer (GEMS) and Pandora measurements, *Atmos. Meas. Tech.*, 16, 3959–3972, <https://doi.org/10.5194/amt-16-3959-2023>, 2023.
- 725 Liu, O., Li, Z., Lin, Y., Fan, C., Zhang, Y., Li, K., Zhang, P., Wei, Y., Chen, T., Dong, J., and De Leeuw, G.: Evaluation of the first year of Pandora NO₂ measurements over Beijing and application to satellite validation, *Gases/Remote Sensing/Validation and Intercomparisons*, <https://doi.org/10.5194/amt-2023-177>, 2023.
- 730 Nawaz, M. O., Johnson, J., Yarwood, G., de Foy, B., Judd, L., and Goldberg, D. L.: An intercomparison of satellite, airborne, and ground-level observations with WRF–CAMx simulations of NO₂ columns over Houston, Texas, during the September 2021 TRACER-AQ campaign, *Atmos. Chem. Phys.*, 24, 6719–6741, <https://doi.org/10.5194/acp-24-6719-2024>, 2024.



- 735 Nowlan, C. R., Liu, X., Janz, S. J., Kowalewski, M. G., Chance, K., Follette-Cook, M. B., Fried, A., González Abad, G., Herman, J. R., Judd, L. M., Kwon, H.-A., Loughner, C. P., Pickering, K. E., Richter, D., Spinei, E., Walega, J., Weibring, P., and Weinheimer, A. J.: Nitrogen dioxide and formaldehyde measurements from the GEOstationary Coastal and Air Pollution Events (GEO-CAPE) Airborne Simulator over Houston, Texas, *Atmos. Meas. Tech.*, 11, 5941–5964, <https://doi.org/10.5194/amt-11-5941-2018>, 2018.
- 740 Park, J.-U., Park, J.-S., Diaz, D. S., Gebetsberger, M., Müller, M., Shalaby, L., Tiefengraber, M., Kim, H.-J., Park, S. S., Song, C.-K., and Kim, S.-W.: Spatiotemporal inhomogeneity of total column NO₂ in a polluted urban area inferred from TROPOMI and Pandora intercomparisons, *GIScience & Remote Sensing*, 59, 354–373, <https://doi.org/10.1080/15481603.2022.2026640>, 2022.
- 745 Reed, A. J., Thompson, A. M., Kollonige, D. E., Martins, D. K., Tzortziou, M. A., Herman, J. R., Berkoff, T. A., Abuhassan, N. K., and Cede, A.: Effects of local meteorology and aerosols on ozone and nitrogen dioxide retrievals from OMI and pandora spectrometers in Maryland, USA during DISCOVER-AQ 2011, *J Atmos Chem*, 72, 455–482, <https://doi.org/10.1007/s10874-013-9254-9>, 2015.
- 750 Schroeder, J. R., Crawford, J. H., Fried, A., Walega, J., Weinheimer, A., Wisthaler, A., Müller, M., Mikoviny, T., Chen, G., Shook, M., Blake, D. R., Diskin, G., Estes, M., Thompson, A. M., Lefter, B. L., Long, R., and Mattson, E.: Formaldehyde column density measurements as a suitable pathway to estimate near-surface ozone tendencies from space, *J. Geophys. Res. Atmos.*, 121, 13,088–13,112, <https://doi.org/10.1002/2016JD025419>, 2016.
- 755 Spinei, E., Whitehill, A., Fried, A., Tiefengraber, M., Knepp, T. N., Herndon, S., Herman, J. R., Müller, M., Abuhassan, N., Cede, A., Richter, D., Walega, J., Crawford, J., Szykman, J., Valin, L., Williams, D. J., Long, R., Swap, R. J., Lee, Y., Nowak, N., and Poche, B.: The first evaluation of formaldehyde column observations by improved Pandora spectrometers during the KORUS-AQ field study, *Atmos. Meas. Tech.*, 11, 4943–4961, <https://doi.org/10.5194/amt-11-4943-2018>, 2018.
- 760 Spinei, E., Tiefengraber, M., Müller, M., Gebetsberger, M., Cede, A., Valin, L., Szykman, J., Whitehill, A., Kotsakis, A., Santos, F., Abuhassan, N., Zhao, X., Fioletov, V., Lee, S. C., and Swap, R.: Effect of polyoxymethylene (POM-H Delrin) off-gassing within the Pandora head sensor on direct-sun and multi-axis formaldehyde column measurements in 2016–2019, *Atmos. Meas. Tech.*, 14, 647–663, <https://doi.org/10.5194/amt-14-647-2021>, 2021.
- 765 Szykman, J., Swap, R., Leffer, B., Valin, L., Lee, S. C., Fioletov, V., Zhao, X., Davis, J., Williams, D., Abuhassan, N., Shalaby, L., Cede, A., Tiefengraber, M., Müller, M., Kotsakis, A., Santos, F., and Robinson, J.: Connecting in-situ and Satellite Monitoring in Support of the Canada – U.S. Air Quality Agreement, *Environmental Managers magazine*, Air & Waste Management Association, 1–7, available at: <https://pubs.awma.org/flip/EM-June-2019/szykman.pdf> (last access: 27 Sep 2023), 2019.
- 770

Szykman, J. J. and Liu, X.: Level 2 Science Data Product Validation Plan, 2023.



- 775 Tirpitz, J.-L., Frieß, U., Hendrick, F., Alberti, C., Allaart, M., Apituley, A., Bais, A., Beirle, S.,
Berkhout, S., Bogner, K., Bösch, T., Bruchkouski, I., Cede, A., Chan, K. L., Den Hoed, M.,
Donner, S., Drosoglou, T., Fayt, C., Friedrich, M. M., Frumau, A., Gast, L., Gielen, C., Gomez-
Martín, L., Hao, N., Hensen, A., Henzing, B., Hermans, C., Jin, J., Kreher, K., Kuhn, J., Lampel,
J., Li, A., Liu, C., Liu, H., Ma, J., Merlaud, A., Peters, E., Pinardi, G., Piters, A., Platt, U.,
Puentedura, O., Richter, A., Schmitt, S., Spinei, E., Stein Zweers, D., Strong, K., Swart, D., Tack,
F., Tiefengraber, M., Van Der Hoff, R., Van Roozendaal, M., Vlemmix, T., Vonk, J., Wagner, T.,
780 Wang, Y., Wang, Z., Wenig, M., Wiegner, M., Wittrock, F., Xie, P., Xing, C., Xu, J., Yela, M.,
Zhang, C., and Zhao, X.: Intercomparison of MAX-DOAS vertical profile retrieval algorithms:
studies on field data from the CINDI-2 campaign, *Atmos. Meas. Tech.*, 14, 1–35,
<https://doi.org/10.5194/amt-14-1-2021>, 2021.
- 785 Travis, K. R., Judd, L. M., Crawford, J. H., Chen, G., Szykman, J., Whitehill, A., Valin, L. C.,
Spinei, E., Janz, S., Nowlan, C. R., Kwon, H., Fried, A., and Walega, J.: Can Column
Formaldehyde Observations Inform Air Quality Monitoring Strategies for Ozone and Related
Photochemical Oxidants?, *JGR Atmospheres*, 127, <https://doi.org/10.1029/2022JD036638>, 2022.
- 790 Tzortziou, M., Herman, J. R., Cede, A., and Abuhassan, N.: High precision, absolute total column
ozone measurements from the Pandora spectrometer system: Comparisons with data from a
Brewer double monochromator and Aura OMI, *J. Geophys. Res.*, 117, 2012JD017814,
<https://doi.org/10.1029/2012JD017814>, 2012.
- 795 Tzortziou, M., Kwong, C. F., Goldberg, D., Schiferl, L., Commane, R., Abuhassan, N., Szykman,
J. J., and Valin, L. C.: Declines and peaks in NO₂ pollution during the
multiple waves of the COVID-19 pandemic in the New York metropolitan area, *Atmos. Chem.
Phys.*, 22, 2399–2417, <https://doi.org/10.5194/acp-22-2399-2022>, 2022.
- 800 Tzortziou, M., Loughner, C. P., Goldberg, D. L., Judd, L., Nauth, D., Kwong, C. F., Lin, T., Cede,
A., and Abuhassan, N.: Intimately tracking NO₂ pollution over the New York City - Long Island
Sound land-water continuum: An integration of shipboard, airborne, satellite observations, and
models, *Science of The Total Environment*, 897, 165144,
<https://doi.org/10.1016/j.scitotenv.2023.165144>, 2023.
- 805 Veeffkind, J. P., Aben, I., McMullan, K., Förster, H., De Vries, J., Otter, G., Claas, J., Eskes, H. J.,
De Haan, J. F., Kleipool, Q., Van Weele, M., Hasekamp, O., Hoogeveen, R., Landgraf, J., Snel,
R., Tol, P., Ingmann, P., Voors, R., Kruizinga, B., Vink, R., Visser, H., and Levelt, P. F.:
TROPOMI on the ESA Sentinel-5 Precursor: A GMES mission for global observations of the
atmospheric composition for climate, air quality and ozone layer applications, *Remote Sensing of
Environment*, 120, 70–83, <https://doi.org/10.1016/j.rse.2011.09.027>, 2012.
- 810 Verhoelst, T., Compennolle, S., Pinardi, G., Lambert, J.-C., Eskes, H. J., Eichmann, K.-U., Fjæraa,
A. M., Granville, J., Niemeijer, S., Cede, A., Tiefengraber, M., Hendrick, F., Pazmiño, A., Bais,
A., Bazureau, A., Boersma, K. F., Bogner, K., Dehn, A., Donner, S., Elokhov, A., Gebetsberger,
M., Goutail, F., Grutter De La Mora, M., Gruzdev, A., Gratsea, M., Hansen, G. H., Irie, H., Jepsen,
N., Kanaya, Y., Karagkiozidis, D., Kivi, R., Kreher, K., Levelt, P. F., Liu, C., Müller, M., Navarro
Comas, M., Piters, A. J. M., Pommereau, J.-P., Portafaix, T., Prados-Roman, C., Puentedura, O.,



- 815 Querel, R., Remmers, J., Richter, A., Rimmer, J., Rivera Cárdenas, C., Saavedra De Miguel, L., Sinyakov, V. P., Stremme, W., Strong, K., Van Roozendael, M., Veefkind, J. P., Wagner, T., Wittrock, F., Yela González, M., and Zehner, C.: Ground-based validation of the Copernicus Sentinel-5P TROPOMI NO₂ measurements with the NDACC ZSL-DOAS, MAX-DOAS and Pandonia global networks, *Atmos. Meas. Tech.*, 14, 481–510, <https://doi.org/10.5194/amt-14-481-2021>, 2021.
- 820 Vigouroux, C., Langerock, B., Bauer Aquino, C. A., Blumenstock, T., Cheng, Z., De Mazière, M., De Smedt, I., Grutter, M., Hannigan, J. W., Jones, N., Kivi, R., Loyola, D., Lutsch, E., Mahieu, E., Makarova, M., Metzger, J.-M., Morino, I., Murata, I., Nagahama, T., Notholt, J., Ortega, I., Palm, M., Pinardi, G., Röhling, A., Smale, D., Stremme, W., Strong, K., Sussmann, R., Té, Y., Van Roozendael, M., Wang, P., and Winkler, H.: TROPOMI–Sentinel-5 Precursor formaldehyde validation using an extensive network of ground-based Fourier-transform infrared stations, *Atmos. Meas. Tech.*, 13, 3751–3767, <https://doi.org/10.5194/amt-13-3751-2020>, 2020.
- 830 Wang, S., Pongetti, T. J., Sander, S. P., Spinei, E., Mount, G. H., Cede, A., & Herman, J.: Direct Sun Measurements of NO₂ column abundances from Table Mountain, California: Intercomparison of low-and high-resolution spectrometers. *Journal of Geophysical Research, Atmosphere* 115, D13305. <https://doi.org/10.1029/2009JD013503>, 2010.
- Wang, B., Geddes, J. A., Adams, T. J., Lind, E. S., McDonald, B. C., He, J., Harkins, C., Li, D., and Pfister, G. G.: Implications of Sea Breezes on Air Quality Monitoring in a Coastal Urban Environment: Evidence From High Resolution Modeling of NO₂ and O₃, *Journal of Geophysical Research: Atmospheres*, 128, e2022JD037860, <https://doi.org/10.1029/2022JD037860>, 2023.
- 835 Yang, L. H., Jacob, D. J., Colombi, N. K., Zhai, S., Bates, K. H., Shah, V., Beaudry, E., Yantosca, R. M., Lin, H., Brewer, J. F., Chong, H., Travis, K. R., Crawford, J. H., Lamsal, L. N., Koo, J.-H., and Kim, J.: Tropospheric NO₂ vertical profiles over South Korea and their relation to oxidant chemistry: implications for geostationary satellite retrievals and the observation of NO₂ diurnal variation from space, *Atmos. Chem. Phys.*, 23, 2465–2481, <https://doi.org/10.5194/acp-23-2465-2023>, 2023.
- 840 Zoogman, P., Liu, X., Suleiman, R. M., Pennington, W. F., Flittner, D. E., Al-Saadi, J. A., Hilton, B. B., Nicks, D. K., Newchurch, M. J., Carr, J. L., Janz, S. J., Andraschko, M. R., Arola, A., Baker, B. D., Canova, B. P., Chan Miller, C., Cohen, R. C., Davis, J. E., Dussault, M. E., Edwards, D. P., Fishman, J., Ghulam, A., González Abad, G., Grutter, M., Herman, J. R., Houck, J., Jacob, D. J., Joiner, J., Kerridge, B. J., Kim, J., Krotkov, N. A., Lamsal, L., Li, C., Lindfors, A., Martin, R. V., McElroy, C. T., McLinden, C., Natraj, V., Neil, D. O., Nowlan, C. R., O’Sullivan, E. J., Palmer, P. I., Pierce, R. B., Pippin, M. R., Saiz-Lopez, A., Spurr, R. J. D., Szykman, J. J., Torres, O., Veefkind, J. P., Veihelmann, B., Wang, H., Wang, J., and Chance, K.: Tropospheric emissions: Monitoring of pollution (TEMPO), *Journal of Quantitative Spectroscopy and Radiative Transfer*, 186, 17–39, <https://doi.org/10.1016/j.jqsrt.2016.05.008>, 2017.
- 850